



Adsorption of BR46 dye using raw and purified clay

A. Bennani Karim^{1,2}, B. Mounir^{1*}, M. Hachkar¹, M. Bakasse³, Z. Rais⁴ and A. Yaacoubi²

^[1] The team of research Analysis, Checks and Environment, high School of Technology, University Cadi Ayyad, BP 89, Safi, Morocco.

^[2] The team Environmental and Experimental Methodology, Laboratory of Organic Applied Chemistry, Faculty of the Sciences Semlalia, BP 2390, Marrakech, Morocco.

^[3] The team of Analysis of the Microphones Polluting Organic, Faculty of the Sciences, University Chouaib Doukkali, BP 20, El jadida, Morocco.

^[4] Industrial effluents team: characterization and treatment, electrochemistry laboratory, modeling and environment engineering LIEME-FSDM-FÈS

* Corresponding author. E-mail address: asmaabennani@yahoo.fr

The adsorption behaviour of Basic Red 46 (BR46) from aqueous solution onto raw (RA) and Purified (PA) natural adsorbent samples was investigated as a function of parameters such as initial dye concentration, contact time and temperature. The Langmuir, Freundlich and Dubinin–Radushkevich (D–R) adsorption models were applied to describe the equilibrium isotherms. The Langmuir monolayer adsorption capacities of RA and PA were estimated at 54 mg/g and 72 mg/g, respectively. The mean adsorption energy derived from D–R isotherm for the PA and the RA showed that the type of adsorption of dye molecules on these materials may be defined as physical adsorption for the PA and ion-exchange processes for the RA. The adsorption rate was fast and the equilibrium was achieved within 20 min at the room temperature. The pseudo-first-order and pseudo-second-order kinetic were used to describe the kinetic data and rate constants were evaluated. The trend of the correlation coefficients values (r^2) were pseudo-second-order > pseudo-first-order. Thermodynamic parameters were also evaluated and revealed that the adsorption process is exothermic in nature. The quite high adsorption capacity of PA will provide an important advantage for using of this material in basic dye solution.

Received: 18 September 2017

Accepted: 12 December 2017

Available online: 12 December 2017

Keywords:

BR46 dye,
Moroccan raw clay,
Moroccan purified clay,
Adsorption,
Isotherms,
Thermodynamic parameters
Adsorption kinetics.

Introduction

Textile dyeing industry is an intensive water consumer and thus, generates high volumes of wastewaters [1]. Dye house effluents contain the unfixed dyes on fibres, auxiliary dyeing chemicals, salts, acids, bases, chlorinated compounds and occasionally heavy

metals [2,3]. These wastewaters are highly variable in composition due to the existence of different cloths, the huge variety of dyes available commercially and fashion trends of each season. In general, these 4 effluents are characterized by high organic content, low biodegradability, variable pH values, low suspended solids content and presence of color. If not

adequately treated, these effluents can originate strong negative impacts on water resources. The input of dyes in aqueous streams changes the natural color, limits water uses (abstraction of drinking water, recreation), affects sunlight penetration and photosynthesis, and can present a toxic effect to aquatic life [3].

Dyes bring us a colorful world, but most dyes have aromatic rings in their structures, which make them highly toxic, carcinogenic, non-biodegradable and mutagenic for human being and aquatic life. According to statistics, all dyes expenditures of textile industries in the world are in excess of 107 kg/year [4; 5]

Several methodologies have been proposed to diminish the content of colorant of wastewater such as membrane separation, flocculation-coagulation, ozonation, oxidation, sedimentation, reverse osmosis, flotation, precipitation, and aerobic or anaerobic treatment [6, 7]. However, the most of them are infeasible due to their high cost or low efficiency. The adsorption is a usual method to the treatment of wastewater for dye removal due to the availability of adsorbents, its simplicity in operation and high efficiency [7].

The most efficient methods are technologies based on adsorption from water onto activated carbon, which appears to be the best method of eliminating of dye. However, this process is expensive and difficult to regenerate after use. Therefore, inexpensive and effective alternative adsorbents are required, and many studies have been devoted to this search. Various types of adsorbents were tested for dye removal and include mineral or organic materials of natural and anthropogenic origin [8, 9, 10]. Among them, clay minerals are an inorganic alternative adsorbent that provides several advantages, which includes its low-cost, abundant availability, non-toxicity and high potential of pollutant adsorption.

The aim of the present study is to investigate the adsorption behaviour of a basic dye onto raw and purified natural adsorbent samples. Basic Red 46 was selected as the modelled basic dye for this work as it is used in textile dying process [11 -12]. The comparison between adsorption isotherms of the basic dye 46 on both PA and RA is significant. The efficiency of PA in the adsorption of BR46 dye was investigated by determining their equilibrium sorption isotherm at various dye concentrations, pH and adsorbent doses.

Material and methods

1. Materials

1.1. Preparation of RA

The raw adsorbent (RA) used in this work is collected from a natural basin in the region of Safi (Morocco), crushed and sieved to 0.08 - 0.1 μm size fractions. Then, it was dried at 378 K (105°C) for 24h and used for further experiments. The main impurities are quartz, dolomite and calcite. RA had a mineral composition of 18% illite, 29% kaolinite and 32% quartz [12].

1.2. Preparation of PA

The < 2 μm fraction was separated by sedimentation. The RA having fraction <80 μm was then saturated with sodium ions by stirring in a 0.1M sodium chloride solution. This was done in triplicate. The saturation was achieved and this suspension was then separated by centrifugation at 3000 r.p.m for 15 min and washed several times with deionised water till no chloride was detected in the centrifuge on titrating with 0.1N AgNO_3 solution. To dissolve carbonates, the Na^+ saturated RA was dispersed in 100 cm^3 of 1 N sodium acetate acetic acid buffer (pH = 4.8). The slurry was stirred to remove carbonates. The Na^+ saturated RA, free from carbonates, is put in suspension in a series of graduated cylinder and the fraction < 2 μm was separated by sedimentation using the Stokes equation. Thereafter, the Na-purified adsorbent (PA) was centrifuged and dried at 373 K (100°C).

1.3. Characterization of the RA and the PA:

The chemical composition of the adsorbent was determined by using Philips X' Cem X-ray fluorescence spectrometer (XRF). The results are given in Table 1.

Tab. 1: Mineralogical composition of RA and PA

	Raw clay	Purified clay
Oxydes	Percentage %	Percentage %
SiO_2	54,76	49,13
Al_2O_3	27,97	34,53
Fe_2O_3	3,22	4,84
CaO	2,83	1,12
MgO	5,07	4,55
SO_3	0,11	0,17
K_2O	3,93	4,19
Na_2O	1,20	0,55
P_2O_5	0,09	0,13

Mineralogical identification was performed by XRD in Siemens D500 diffractometer using a 106 $\text{CuK}\alpha$ radiation ($\lambda = 1.5406 \text{ \AA}$), produced under conditions of 40 kV and 20 mA.

1.4. Adsorbate

The basic dye used as adsorbate in the present study is basic red BR46 which is purchased from SDI textile company (Safi, Morocco). His molecular weight is 357.5 g mol^{-1} .

2. Methods

2.1. Adsorption studies

In adsorption experiments, a 0.04 g of adsorbent sample and Basic Red 46 concentration of 20 mg/dm^3 were kept constant. At the end of each adsorption period, the supernatant was centrifuged for 4 min at 2500 r.p.m. The concentration of Basic Red 46 remaining in the supernatant after and before adsorption was determined with a 1.0 cm light path quartz

cells using spectrophotometer [GBC (ajax, ontario) UV/visible 911] at λ_{\max} of 530 nm. The adsorbed amount of BR46 was calculated from the concentrations in solution before and after adsorption. A linear correlation was established between the dye concentration and the absorbance at λ_{\max} = 530 nm, in the range $C_{\text{dye}}=0-28 \text{ mg/dm}^3$ with a correlation coefficient $r^2 = 0.99$. The adsorption capacity of the BR46 dye was calculated as follows: $q_t = [(C_0 - C_t) V]/W$. Where q_t (mg/g) is the amount of BR46 adsorbed at contact time t (min), C_0 (mole dm^{-3}) is the initial dye concentration, C_t is the dye concentration at time t , and W (g) is the adsorbent amount in the solution. All experiments were always performed in duplicates. $\pm 5\%$ was the experimental error limit of each duplicates, Time to attain equilibration between solution and adsorbent was chosen as 70 min, despite the fact that the studies related to kinetics implied a shorter time than this duration (see below).

2.2. Effect of initial dye concentration:

The effect of the initial dye concentration was investigated as follows: 0.04g sample of adsorbent was added to 100 cm^3 solution of BR46 with initial concentrations varying from 10 to 28 mg/dm^3 .

2.3. Effect of adsorbent mass:

The effect of varying the adsorbent mass on dye adsorption were carried out by adding 10, 20, 40, 50, and 60 mg samples of adsorbent to 100 cm^3 solution of BR46 aqueous solution having an initial dye concentration of 20 mg/dm^3 .

2.4. Effect of temperature:

Temperature effect on adsorption for determination of thermodynamic parameters was studied for four temperatures: 303, 313, 323 and 333 K. A sample of 0.04 g of adsorbent was added to dye solution (100 cm^3 , 20 mg/dm^3) at pH= 6. The experiments were carried out in a constant temperature shaker bath.

Results and discussion

1. Characterization of adsorbent:

The RA and the PA have been characterized mineralogically (X-ray diffraction) and chemically (oxides composition). The RA and the PA compositions are presented in Table 1. The results of chemical analysis show that the SiO_2 and Al_2O_3 are the major constituents of the adsorbents with other oxides present in trace amounts. A most important reduction of calcium is observed in the PA in comparison with the RA, this indicate that the calcium comes mainly from carbonates.

The mineralogical composition of the RA and the PA was determined from X-ray diffractogram (Figure 1). The predominant peaks found for the RA were 9.99, 7.16, 5.02, 4.47, 4.25, 3.579, 3.34, 3.03 and 2.9 Å which correspond to illite, kaolinite, illite, kaolinite, quartz, kaolinite, quartz+illite, calcite and dolomite. XRD

patterns of PA (particles < 2 μm) fraction show a most important reduction in the peaks characteristics of quartz, dolomite and calcite (Figure 1). Moreover, the peaks of illite and kaolinite became more intense (9.99, 7.16, 5.02 and 4.47 Å).

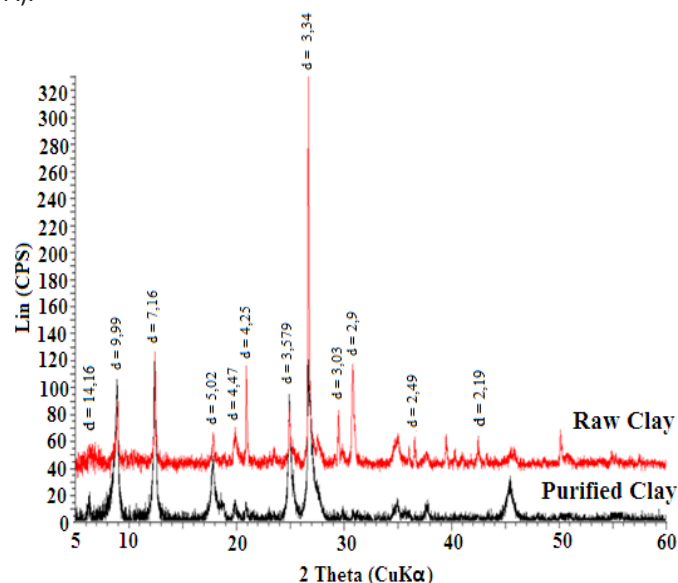


Fig. 1: X-ray diffractometer analysis for the natural adsorbent RA and the $\leq 2\mu\text{m}$ fraction PA

2. Effect of adsorbent amount

The BR46 adsorption onto RA and the PA was studied by changing the amount of adsorbent (20, 30, 40, 50, and 60 mg /100 cm^3) in the test solution while keeping the initial dye concentration (20 mg/dm^3) constant, at different contact times during 120 min. For both systems, it was observed that the uptake of the dye increased by increasing adsorbent amount from 20 to 40 mg, thus, the residual concentration decrease (Fig 2). The further increase in the adsorbent amount did not affect the uptake capacity significantly [13]. Increase in the adsorption with adsorbent dose can be attributed to increased adsorbent surface area and availability of more adsorption sites [14, 15]. At lower adsorbent dosage, a majority of active sites of adsorbent are exposed and utilized [1, 16]. At higher adsorbent dosage, the active sites are much more than the saturated threshold adsorption point, and available CR molecules were insufficient to cover all the active sites. Both of the reasons result in the increase in removal efficiencies. We note that maximum dye removal was achieved within adsorbent amount of 40 mg. This weight was then chosen for all further studies. We note also that the BR46 dye adsorption on the PA is slightly effective compared to that of the RA, due to the fact that the PA has more clay fraction of kaolinite and illite, less silice compared to the RA.

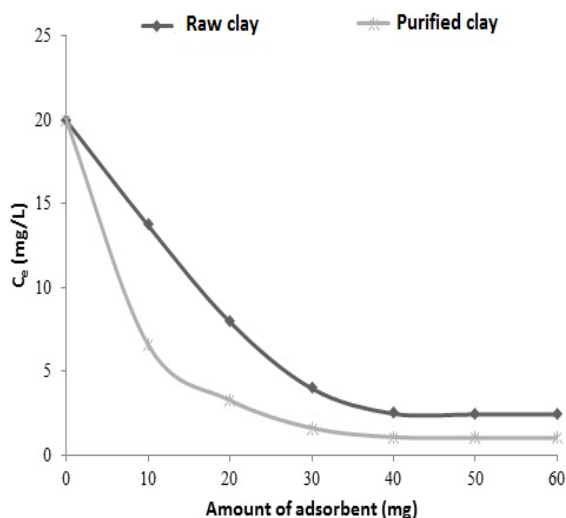


Fig. 2 : Effect of adsorbent amount (10 mg, 20 mg, 40 mg, 50 mg, 60 mg, $t_{eq} = 2$ h). on the equilibrium concentrations of BR46 adsorbed onto RA and PA achieved with initial dye concentration of 20 mg/dm³. (♦: RA, ■: PA)

3. Effect of contact time and initial dye concentration

The removal of dye was rapid in the initial stages of contact time and gradually decreased with time until equilibrium (Fig. 3). The rapid adsorption observed during the first 10 min is probably due to the abundant availability of active sites on the clay surface, and with the gradual occupancy of these sites, the sorption becomes less efficient. It appears from Fig. 3 that the contact time needed to reach equilibrium conditions was 20 to 25 min. This is in accordance with the results obtained in different types of adsorbents as for example dye adsorption experiments onto surfactant-treated aluminum/chromium- intercalated bentonite [17], kaolinite [18], it was clear that the removal of dye was dependent on the concentration of the dye. The adsorption capacity increased with increasing initial dye concentration and the process was faster at higher concentrations.

The influence of contact time on removal of BR46 by RA and PA at pH 6 and 293 K (20 °C) is shown in Fig 3 (a et b). It is evident that both materials are efficient to adsorb dye. The dye adsorption of the PA sample is faster than that of RA sample. Moreover, the maximum amount of adsorbed dye (q_e) is higher for the PA sample (24.44, 38.43 and 55.46 mg/g) than for the RA sample (23.25, 34.61 and 45.80 mg/g) for the concentrations: 10; 16; 24 mg/dm³ respectively (Table 2). The increase in concentration of BR46 increases the extent of adsorption; this indicates that the initial dye concentration plays an important role in the adsorption capacity of dye [19]. To reach equilibrium, it takes 20 min for both PA and RA. The adsorption capacity of adsorbents with respect to equilibrium time is in concordance with the order of the structure heterogeneity (PA > RA) and perhaps the surface area (PA > RA) [17].

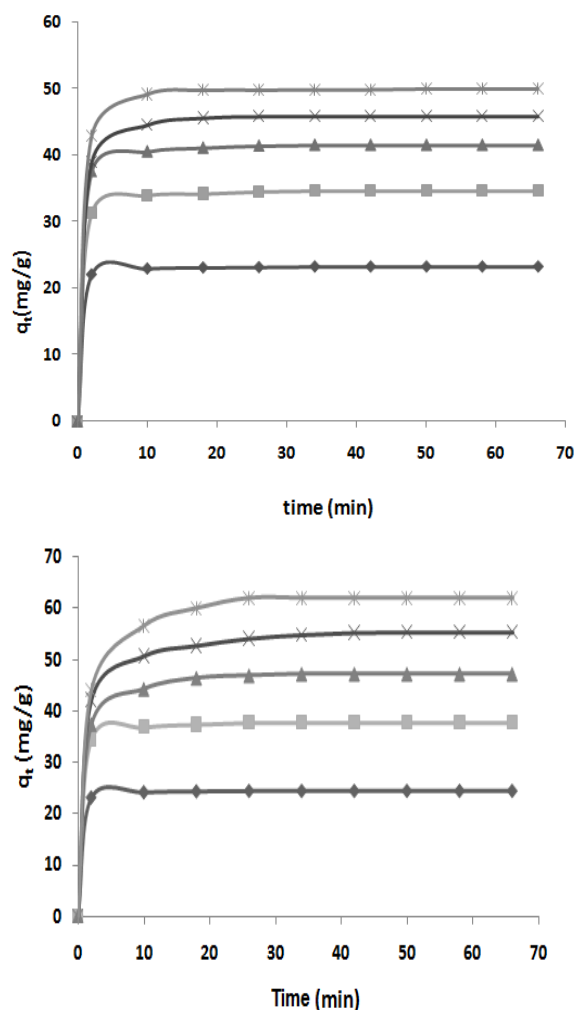


Fig. 3: Kinetic curves of BR46 retention by the (a): RA, (b): PA at different initial BR46 concentrations (♦:10 mg/dm³, ■: 16 mg/dm³, ▲: 20 mg/dm³, ×: 24 mg/dm³, *: 28 mg/dm³).

4. Kinetic of adsorption process:

The kinetic study of the adsorption processes provides useful data regarding the efficiency of adsorption and feasibility of scale-up operations.

Kinetic of the interaction between the RA, PA and the BR46 dye is studied by applying the following equations and models. Firstly, Lagergren equation is applied, assuming pseudo-first-order kinetic, where the number of dye ions is greater than the number of adsorption sites on adsorbent surfaces [17]. To evaluate the effectiveness of an adsorbate, equilibria adsorption kinetic studies are needed.

Adsorption kinetics are used in order to explain the adsorption mechanism and adsorption characteristics.

Tab. 2: Kinetics parameters for the effect of solution concentrations on RA and PA

C (mg/L)		q_{eexp} (mg/g)	Pseudo 1 ^{er} ordre			Pseudo 2 ^{eme} ordre		
			q_e (mg/g)	K_1 (min ⁻¹)	r^2	q_e (mg/g)	K_2 (g/mg.in)	r^2
RA	10	23,25	4,35	0,16	0,67	23,31	0,32	0,99
	16	34,61	7,29	0,11	0,5	34,72	0,12	0,99
	24	45,80	14,13	0,17	0,8	46,08	0,084	0,99
PA	10	24,44	6,95	0,26	0,8	24,5	0,42	0,99
	16	38,43	15,24	0,2	0,8	37,87	0,13	0,99
	24	55,46	32,24	0,14	0,9	56,17	0,019	0,99

4.1. Pseudo-first-order reaction kinetic

The adsorption rate constant proposed by Ho [20] using first order reaction kinetic is shown below:

$$dq_t/dt = k_1(q_e - q_t)$$

Where k_1 is the adsorption rate constant for the first order adsorption (min⁻¹), q_t is the amount of dye adsorbed at time t (mg/g) and q_e is the amount of dye adsorbed at saturation (mg/g). The integration of the Eq. (13) gives the following expression:

$$\ln(q_e - q_t) = -k_1 t + C_1 \quad (1)$$

Where C_1 is the integration constant for first order reaction kinetic.

If it is supposed that $q=0$ at $t=0$, then:

$$\ln(q_e - q_t) = \ln q_e - k_1 t \quad (2)$$

The values of k_1 can be obtained from the slope of the plot of $\ln(q_e - q_t)$ vs. time. The validity of the first-order kinetics and hence the Lagergren equation can be tested by comparing theoretical q_e values obtained from the intercepts with the experimental ones. If the validity is less, the kinetics can be tested again for the following second-order mechanism.

4.2. Pseudo-second-order reaction kinetic

Adsorption data was also evaluated according to the Pseudo second-order reaction kinetic proposed by Ho and Ugurlu [20, 21]

$$dq_t/dt = k_2(q_e - q_t)^2 \quad (3)$$

where k_2 is the second order reaction constant. If Eq. (3) is integrated, the following expression is obtained:

$$1/(q_e - q_t) = k_2 t + C_2 \quad (4)$$

In Eq. (4), C_2 is the integration constant of the second order reaction kinetic. With an algorithmic arrangement, the following statement is formed:

$$t/q_t = 1/K_2 q_e^2 + t/q_e \quad (5)$$

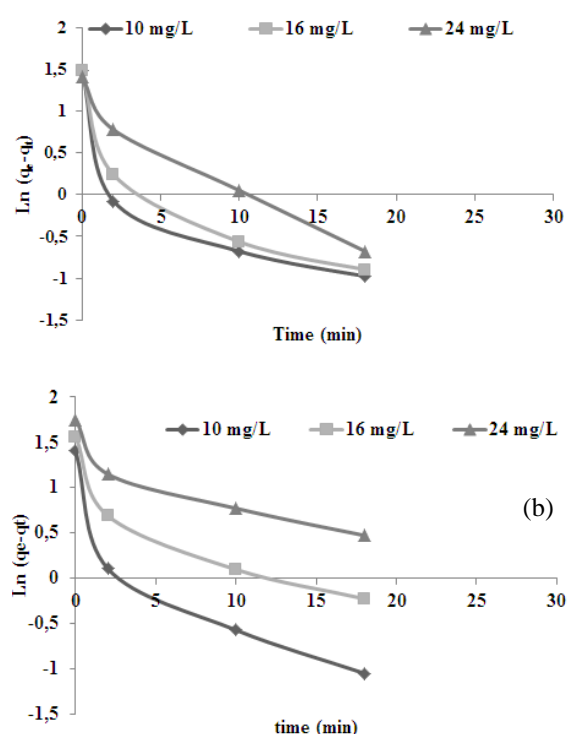
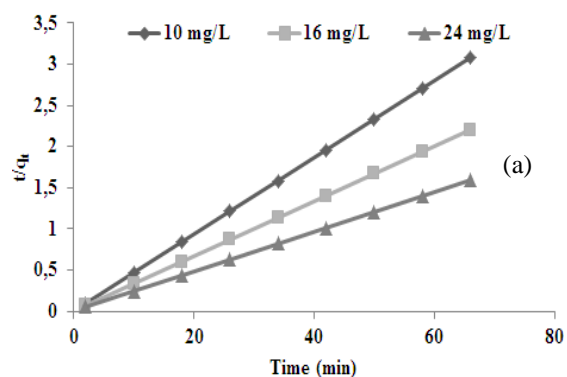
In the study, the initial BR46 concentrations were determined as 10, 16, 24 mg/L. The dependences of these concentrations against time are shown in Fig. 5.

In order to calculate the adsorption rate constants of BR46, the first order reaction kinetic was applied, it is seen that the curves in the plots of $\ln(q_e - q_t)$ against time, are not linear. First order reaction kinetics for BR46 adsorption onto raw and purified clay are shown in Fig. 4 (a and b). Rate constants (k_1) were calculated from the slopes of the curves (Table 2).

Pseudo-second-order kinetic was also applied for the experimental data of dye.

The curves in the plot of t/q_t against t are linear and k_2 (g/mg min) rate constants can be calculated from the slope of these curves (Fig. 5 (a and b)).

The validity of the model can also be tested by comparing obtained values of q_e to the experiment values.

**Fig. 4.:** Pseudo-first order reaction kinetics for the adsorption of BR46 on natural (a) raw and (b) purified clay.

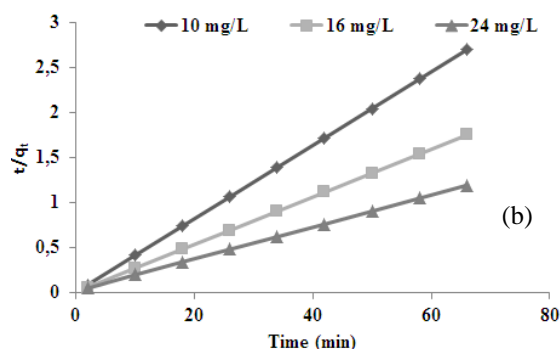


Fig. 5: Pseudo-second order reaction kinetics for the adsorption of BR46 on natural (a) raw and (b) purified clay.

In order to quantify the applicability of each model, the correlation coefficients (r^2) were calculated. The analyses of the correlation coefficients (r^2) showed that the experimental data ($r^2 \approx 0.99$) fit to the pseudo-second order model better than to the pseudo-first-order model for the raw and purified clay ($r^2 < 0.90$) (Table 2). While the calculated equilibrium sorption capacity values for the first order model for all initial concentrations, $q_{e,calc}$, are not close to the experimental values ($q_{e,exp}$). For the second-order model, $q_{e,calc}$ values are close to $q_{e,exp}$ for all initial concentrations (Table 2) [17, 20]. However, the values of the rate constants (K_2) were found to decrease from 0.32 to 0.084 g mg⁻¹ min⁻¹ as the initial concentration increased from 10 to 24 mg dm⁻³ for the RA and from 0.42 to 0.019 for the PA, showing the process to be highly concentration dependent, which is consistent with earlier studies [20–22]. The correlation coefficients for pseudo-second order (r^2) were higher than 0.95 for all initial concentrations. These findings show that kinetics of dye adsorption by PA and RA are better described by pseudo-second-order kinetic model rather than pseudo-first-order model (Table 2) [22].

5. Thermodynamic parameters

The temperature range used in this study varied from 303 to 333 °K at 20 mg/dm³ dye solution concentration having a pH 6. The sorption capacity decreased from 40.54 to 38.91 mg/g for the RA and from 44.99 to 43.79 for the PA indicating that the temperature unfavours the dye adsorption.

The negative value of ΔH° indicates that the process is exothermic in nature, and the negative values of ΔG° show the spontaneous adsorption of reactive dyes on the adsorbent. Moreover, ΔG° is less negative with temperature increase (Table 3) showing that the adsorption process is thermodynamically feasible at room temperature but less with higher temperatures. [15, 23].

The adsorption thermodynamic parameters were determined at different temperatures (303, 313, 323 and 333 K) using the following equations:

$$\ln(k_d) = \Delta S_{ads}/R - \Delta H_{ads}/RT \quad (6)$$

and

$$\Delta G_{ads} = \Delta H_{ads} - T\Delta S_{ads} \quad (7);$$

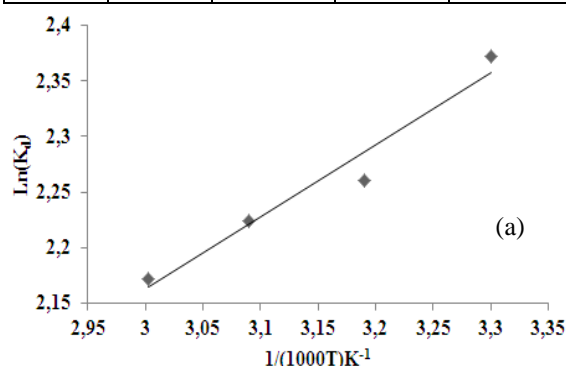
where k_d is the distribution coefficient at different temperature (303 K, 313 K, 323 K and 333 K) and is equal to the ratio of the equilibrium amount adsorbed (q_e in mg/g) to the equilibrium concentration (C_e in mg/dm³) at different temperature ($k_d = q_e / C_e$) and R is the gas constant.

The second equation was applied to calculate the standard Gibbs free energies. The values of ΔS_{ads} and ΔH_{ads} were obtained from the slope and intercept of the linear plot of $\log k_d$ versus $1/T$, respectively (Fig. 6).

For both the RA and the PA, the negative values of ΔG_{ads} (Table 3) indicate that the adsorption of BR46 is spontaneous [12; 23]. The negative values of the enthalpy change (–5.30 kJ/mole) for the RA and (–7.03 kJ/mole) for PA indicate that the adsorption is exothermic. The positive values of ΔS_{ads} show increased randomness at the solid–solution interface during the adsorption of dye onto RA and PA [12, 23].

Tab. 3: Thermodynamic parameters

BR46 (20 mg/L)					
T (°K)		q_e (mg/g)	ΔG° (kJ/mol)	ΔH° (kJ/mol)	ΔS° (kJ/mol K)
RA	303	40,54	-5,85
	313	39,65	-5,87	-5,30	0,002
	323	39,36	-5,89
	333	38,91	-5,91
PA	303	44,99	-7,68
	313	44,34	-7,70	-7,03	0,002
	323	43,95	-7,73



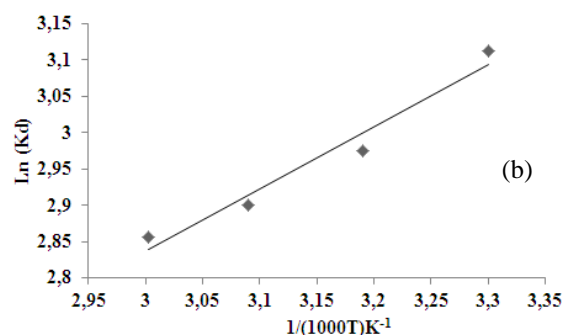


Fig. 6: Van't Hoff plot for the dye adsorption on a: RA, b: PA of the clay ($C = 20 \text{ mg/L}$).

6. Adsorption isotherms

The adsorption isotherms were evaluated using Langmuir, Freundlich and Dubinin- Radushkevich isotherms. The Langmuir and Freundlich models are defined with $C_e/q_e = 1/(q_{\max} * K_a) + C_e/q_{\max}$ (8) and $\text{Log}(q_e) = (1/n) \text{Log}(C_e) + \text{Ln}(K_f)$ (9). Where q_e is the amount adsorbed at equilibrium (mg/g), C_e the equilibrium concentration of the adsorbate (mg/dm³), q_{\max} (mg/g) and K_a (dm³/mg) are the Langmuir constants related to the maximum adsorption capacity and the adsorption energy respectively, $1/n$ is the adsorption intensity, K_f represents the adsorption capacity related to Freundlich isotherm. The Dubinin- Radushkevich (D-R) model was used to find out the constant B_D (mol²/kJ²) related to the sorption energy from $q_e = q_{\max} \exp(-B_D [RT \ln(1 + 1/C_e)]^2)$ (10), where q_e is the amount of BR46 adsorption in (mg/g), q_{\max} (mg/g) is the D-R monolayer capacity, T (°K) is the temperature and C_e (mg/L) is the equilibrium concentration of BR46 solution. The adsorption data were analyzed using the linear form of the D-R isotherm expressed as: $\ln q_e = \ln q_{\max} - B_D \epsilon^2$ (11). Where q_e is the amount adsorbed at equilibrium (mg/g), q_{\max} (mg/g) is the adsorbent monolayer capacity, B_D (mol²/kJ²) is a constant related to sorption energy via the following relationship $E = 1/(2B_D)^{0.5}$ (12), and ϵ is the Polanyi potential, which is related to the equilibrium concentration as $\epsilon = RT \ln(1 + 1/C_e)$ (13).

Another important parameter, R_L , known as the separation factor, could be obtained from the relation: $R_L = 1/(1 + K_L C_0)$ (14); where C_0 is initial concentration (mg/dm³) and K_L is the Langmuir constant (dm³/mg).

6.1. The Langmuir and Freundlich isotherms

To gain further understanding of the behaviour and mechanism of RA and PA with BR46 dye, Langmuir, Freundlich isotherms were studied. The plot of C_e/q_e against C_e (equation 8) gives a straight line confirming that the adsorption of the dye follows the Langmuir isotherm model [24]. On the basis of slopes and intercepts of the straight lines, Langmuir constants were calculated and are presented in Table 4. The validity of Freundlich adsorption model was established using the equation 9. Table 4 reveals that, for the RA and the PA, the Langmuir correlation

coefficient r^2_L is higher than the Freundlich correlation coefficient r^2_F . It indicates that the Langmuir isotherm shows better fit to adsorption than the Freundlich isotherm. Similar observations were reported for adsorption textile dye onto activated sepiolite [21].

Tab. 4: Langmuir, Freundlich and Dubinin Radushkevich parameters

Isotherms models	BR46	
	Raw adsorbent	Purified Adsorbent
Langmuir		
(mg/g)	54,14	71,51
q_0 (mmole/g)	0,12	0,22
K_L (L/mg)	1,19	1,87
R^2	0,99	0,99
R_L	0,27	0,34
Δq %	4	2,95
Freundlich		
K_F (mg/g)	30,50	44,42
n	4,04	3,06
R^2	0,96	0,98
Δq %	9	3,3
Dubinin Radushkevich		
Q_{exp} (mg/g)	47,99	58,22
E (Kj/mol)	10,2	7,37
B_D (mol ² kJ ⁻²)	0,0018	0,0092
R^2	0,91	0,98

The Langmuir monolayer adsorption capacities of RA and PA were estimated as 54 and 72 mg/g, respectively (Table 4). The lower K_F , K_L and q_{\max} values for the RA compared to that for PA (Table 4) indicate that the purification process influences the adsorption equilibrium and PA is more effective in adsorbing dye BR46 than RA. If the value of Freundlich constant n is below unity, the adsorption process is unfavorable, but it is above unity, the adsorption is favorable [22-25]. In the present study, the value of n at equilibrium was above 1 for the two adsorbents, representing favorable adsorption.

For the RA and PA, the R_L values obtained are less than unity (Table 4), confirming that adsorption process is favourable [15, 17].

6.2. Dubinin- Radushkevich isotherm

The mechanism of BR46 adsorption from solution onto adsorbent surface was then examined with the Dubinin-Radushkevich (D-R) equation (10), the isotherm constants are presented in Table 4. The slope and intercept of the plots of $\ln q_e$ versus ϵ^2 give B_D and q_{\max} , respectively. B_D is related to

sorption energy E , via the following relationship $E = 1 / (2B_D)^{0.5}$. The mean adsorption energy is the free energy change when one mole of the ion is transferred to the surface of the solid from infinity in the solution [26]. $E_{DR} \approx 8 \text{ kJ/mole}$ has been assumed as a threshold for definition of the nature of adsorption; the physical forces such as diffusion process is effective on sorption if $E_{DR} < 8 \text{ kJ/mole}$ [27], an energy range from 8 to 16 kJ/mole indicates ion-exchange processes [18]. In the case of $E > 16 \text{ kJ/mole}$, the type of adsorption may be defined as chemical adsorption [22]. The E value of BR46 adsorption by RA was found to be 10.2 kJ/mole, this implies that the type of adsorption is ion-exchange mechanism [22]. For PA, the E value was found to be 7.32 kJ/mole; hence, the type of adsorption of BR46 on the PA may be defined as physical adsorption. The rise in E_{DR} of BR46 for RA in comparison to that for PA was also an evidence for the barrier effect of adsorbent purification on reaching to the adsorptive sites.

Conclusion

The study of the adsorption of a pure organic dye, the BR46 on RA and on PA was undertaken in static mode at 298 °K (25 °C) and under the atmospheric pressure. A comparative adsorption study of BR46 onto RA and PA evidences the high adsorption capacity of dye on the purified adsorbent obtained from adsorption isotherms ($PA > RA$), which are modelled using different isotherm models. The adsorption was rapid and initial dye concentration, adsorbent mass dependent. The Freundlich equation described well the experimental results but less accurate than Langmuir model, the adsorbed amount in the equilibrium reached 72 mg/g for the PA and 54 mg/g for the RA. The kinetic study revealed that approximately 20 minutes of agitation are sufficient to reach a complete equilibrium for the BR46 PA and RA systems. The process of adsorption was best described by the pseudo-second-order rate model. These results generally showed that PA could be considered as a potential adsorbent for BR46 removal from aqueous solutions.

Acknowledgements:

We thank all the staff and professors, who have made me benefit from their scientific knowledge and for having led this work with great interest and patience. I thank the analysis, checks and environment team, high school of technology, the environmental and experimental methodology team, laboratory of organic applied chemistry, and Cadi Ayyad University, for receiving me to achieve this work.

References

1. C.R. Sílvia Santos, A.R. Rui Boaventura, *J. Environ. Chem. Engin.*, 4, 2, **2016**, 1473-1483.
2. G. Crini, P.M. Badot, *Prog Polym Sci*, 33 (2008) 399- 447.

3. C.R. Sílvia Santos; A.R. Rui Boaventura; *J. Hazard. Mater.* 291, **2015**, 74-82
4. V.S. Mane, P.V. Babu, *J. Taiwan Inst. Chem. Eng.* 44, **2013** 81–88.
5. J. Zhou, Q.F. Lü, J.J. Luo; *J. Clean. Prod.*, In press, accepted manuscript, Available online 1 September **2017**.
6. M.T. Yagub, T.K. Sen, S. Afroze, H.M. Ang, *Adv. Colloid Interf. Sci.* 209, **2014**, 172- 184.
7. J.E. Aguiar, J.A. Cecilia, P.A.S. Tavares, D.C.S. Azevedo, I.J. Silva, *Applied Clay Sci.*, 135, **2017**, 35-44.
8. B. Noroozi, G.A. Sorial, *J. Environ. Sci.* 25, **2013**, 419- 429.
9. O.E. Ismail, L. Yildirim, E. Ozdogan, *J. Clean. Prod.* 70, **2014**, 61- 67.
10. N. Abidi, E. Errais, J. Duplay, A. Berez, A. Jrad, G. Schafer, M. Ghazi, K. Semhi, M. Trabelsi-Ayadi, *J. Clean. Prod.*, 86, **2015**, 432-440.
11. N. Yeddou, A. Bensmaili, *Desalination*, 185, **2005**, 499- 508.
12. A. Bennani Karim, B. Mounir, M. Hachkar, M. Bakasse, A. Yaacoubi, *J. Hazard. Mater.* 168, 1, **2009**, 304-309.
13. V.K. Gupta, A. Mittal, V. Gajbe, *J. Colloid Interf. Sci.* 284, **2005**, 89- 98.
14. W.T. Tsai, H.C. Hsu, T.Y. Su, K.Y. Lin, C. Ming Lin, T.H. Dai, *J. Hazard. Mater.* 147, (**2007**), 1056- 1062.
15. D. Kavak, *J. Hazard. Mater.*, 163, **2009**, 308- 314.
16. Y. Li, J. Suna, Q. Dua, L. Zhang, X. Yanga, S. Wua, Y. Xiaa, Z. Wanga, L. Xiaa, A. Cao; *Carbohydr. Polym.* 102, **2014**, 755–761.
17. Z. Boubberka, A. Khenifi, H. Ait Mahamed, B. Haddou, N. Belkaid, N. Bettahar, Z. Derriche, *J. Hazard. Mater.* 162, **2009**, 378- 385.
18. M. Dogan, M. Hamdi Karaoglu, M. Alkan, *J. Hazard. Mater.* 165, **2009**, 1142- 1151.
19. A. Gürses, Ç. Dogar, M. Yalçın, M. Açıkyıldız, R. Bayrak, S. Karaca, *J. Hazard. Mater.* B131, **2006**, 217- 228.
20. Y.S. Ho, *Scientometrics* 59, **2004**, 171- 177.
21. M. Ugurlu, *J. Microp. and Mesop. Materials*, 119, **2009**, 276- 283.
22. E. Eren, *J. Hazard. Mater.* 162, (**2009**) 1355-1363.
23. E. Errais, J. Duplay, F. Darragi, I. MRabet, A. Aubert, F. Huber, G. Morvan, *Desalination* 275, **2011**, 74- 81.
24. M. Bouraada, F. Belhafaoui, M.S. Ouali, L.S. Menorval, *J. Hazard. Mater.*, 163, **2007**, 463- 467.
25. P. Panneer Selvam, S. Preethi, P. Basakaralingam, N. Thinakaran, A. Sivasamy, S. Sivanesan, *J. hazard. Mater.* 155, **2008**, 39- 44.
26. S.S. tahir, N. Rauf, *Chemosphere*, 63, **2006**, 1842- 1848.
27. U. Ulusoy, R. Akkaya, *J. Hazard. Mater.* 163, **2009**, 98- 108.